

# CD4<sup>+</sup>CD25<sup>-</sup> T-Cell-Secreted IFN- $\gamma$ Promotes Corneal Nerve Degeneration in Diabetic Mice

Yujing Lin,<sup>1,2</sup> Lingling Yang,<sup>1,2</sup> Ya Li,<sup>1,2</sup> Shengqian Dou,<sup>1,2</sup> Zhenzhen Zhang,<sup>1,2</sup> and Qingjun Zhou<sup>1,2</sup>

<sup>1</sup>State Key Laboratory Cultivation Base, Shandong Provincial Key Laboratory of Ophthalmology, Eye Institute of Shandong First Medical University, Qingdao, China

<sup>2</sup>Qingdao Eye Hospital of Shandong First Medical University, Qingdao, China

Correspondence: Qingjun Zhou, Qingdao Eye Hospital of Shandong First Medical University, 5 Yan'er Dao Rd., Qingdao 266071, China; [qjzhou2000@hotmail.com](mailto:qjzhou2000@hotmail.com).

Received: August 27, 2024

Accepted: March 17, 2025

Published: April 7, 2025

Citation: Lin Y, Yang L, Li Y, Dou S, Zhang Z, Zhou Q. CD4<sup>+</sup>CD25<sup>-</sup> T-cell-secreted IFN- $\gamma$  promotes corneal nerve degeneration in diabetic mice. *Invest Ophthalmol Vis Sci*. 2025;66(4):15. <https://doi.org/10.1167/iov.66.4.15>

**PURPOSE.** This study aimed to explore the relationship between corneal nerve degeneration and elevated dendritic cells (DCs) in diabetic keratopathy.

**METHODS.** Corneas from diabetic and healthy mice were analyzed using single-cell RNA sequencing. Corneal nerve density and DC and T-cell infiltration were quantified through whole-mount corneal staining. Freshly isolated mouse trigeminal ganglion (TG) neurons were co-cultured with immature DCs, mature DCs, activated CD8<sup>+</sup> T cells, and CD4<sup>+</sup>CD25<sup>-</sup> T cells. TG neurite outgrowth was assessed to identify potential effector cells driving corneal nerve degeneration. In addition, interferon-gamma (IFN- $\gamma$ ) and blocking antibodies were used to evaluate their effects on TG neurite outgrowth and corneal nerve degeneration in mice.

**RESULTS.** Compared with age-matched healthy mice, diabetic mice exhibited a significant reduction in corneal nerve density and sensitivity, along with increased infiltration of DCs, CD4<sup>+</sup> T cells, and CD8<sup>+</sup> T cells. In vitro co-culture experiments revealed that CD4<sup>+</sup>CD25<sup>-</sup> T cells, rather than DCs and CD8<sup>+</sup> T cells, significantly inhibited TG neurite outgrowth. Among cytokines, elevated IFN- $\gamma$  in diabetic corneas impaired TG neurite outgrowth and induced corneal nerve degeneration, whereas IL-4 and IL-17 had no such effect. Blocking IFN- $\gamma$  alleviated CD4<sup>+</sup>CD25<sup>-</sup> T-cell-induced inhibition of TG neurite outgrowth and corneal nerve degeneration in diabetic mice.

**CONCLUSIONS.** CD4<sup>+</sup>CD25<sup>-</sup> T cells, but not DCs or CD8<sup>+</sup> T cells, contribute to corneal nerve degeneration in diabetic mice, a process partially mediated by IFN- $\gamma$ .

**Keywords:** CD4<sup>+</sup>CD25<sup>-</sup> T cells, diabetes mellitus, corneal nerve degeneration, interferon-gamma (IFN- $\gamma$ )

Diabetes mellitus (DM) is a global public health issue, affecting 536.6 million people in 2021, with projections reaching 783.2 million by 2045.<sup>1</sup> As a systemic disease, DM can contribute to severe complications in multiple organs or tissues.<sup>2</sup> Compared with diabetic retinopathy and cataracts, the association between DM and ocular surface diseases remains less understood. However, diabetic keratopathy has been reported in 47% to 64% of patients, although it is often underdiagnosed.<sup>3</sup> Clinical manifestations of diabetic keratopathy include superficial punctate keratitis, delayed epithelial wound healing, tear film alterations, corneal ulceration, and neuropathy characterized by reduced corneal sensitivity.<sup>4,5</sup> Corneal confocal microscopy has confirmed significant alterations in diabetic corneal nerves, including the reduction of density, branches, and length,<sup>6</sup> with variations depending on the neuropathy severity.<sup>7</sup> We and others have investigated the roles of various neurotrophic factors and axon guidance molecules in diabetic corneal epithelium and nerve fiber regeneration.<sup>8–12</sup> However, the direct mechanism by which DM induces corneal nerve degeneration remains unclear.

The cornea has historically been regarded as an immune-privileged tissue; however, recent studies have described a negative correlation between corneal nerves and activated immune cells.<sup>13,14</sup> Several distinct resident immune cells, including dendritic cells (DCs), macrophages, mast cells, and T cells, have been identified in the cornea,<sup>15,16</sup> where they localize adjacent to sensory nerves and play crucial roles in maintaining homeostasis and mediating inflammatory responses.<sup>17</sup> DM significantly alters the composition and function of immune cells in the cornea. In healthy corneas, DCs are primarily located in the limbal and peripheral regions, with decreasing density toward the central region. In diabetic corneas, most studies have confirmed increased corneal DC density in both type 1 and type 2 diabetes,<sup>13,18–20</sup> although a few studies have reported reduced corneal DCs in diabetic mice.<sup>21</sup> During corneal wound healing, DCs are in close proximity to the sensory nerve<sup>22</sup> and can promote diabetic corneal nerve regeneration by secreting ciliary neurotrophic factors.<sup>21</sup> Although most studies have focused on the relationship between DCs and diabetic corneal nerve regeneration, the role and mechanism of DCs

in mediating diabetic corneal nerve degeneration remain unclear.

As antigen-presenting cells, dendritic cells play a crucial role in initiating immune responses by activating primary T lymphocytes under antigen stimulation.<sup>23,24</sup> DCs and adaptive immune cells, including T and B cells, have been implicated in peripheral neurodegeneration.<sup>25</sup> Previous studies have confirmed that CD4<sup>+</sup> T cells contribute to corneal nerve damage in conditions such as herpes simplex virus 1 (HSV-1) infection, graft-versus-host disease, and dry eye disease.<sup>26–28</sup> CD4<sup>+</sup> T cells are further classified based on their cytokine secretion, including Th1 cells producing IFN- $\gamma$ , Th2 cells producing IL-4, and Th17 cells producing IL-17.<sup>29–31</sup> Mass cytometry analysis has found significant alterations in myeloid and T-cell populations in diabetic corneas.<sup>32</sup> However, the involvement of T-cell-mediated adaptive immunity in diabetic corneal nerve degeneration remains incompletely understood.

In the present study, we assessed the alterations of DC and T-cell populations in diabetic mouse corneas using single-cell RNA sequencing (scRNA-seq) and whole-mounted corneal staining. Furthermore, we evaluated the effects of various immune cells and secreted cytokines on trigeminal ganglion (TG) neurite outgrowth and corneal nerve degeneration. Our findings identified CD4<sup>+</sup>CD25<sup>–</sup> T cells, but not DCs and CD8<sup>+</sup> T cells, as contributors to diabetic corneal nerve degeneration through IFN- $\gamma$  secretion.

## MATERIALS AND METHODS

### Animals

C57BL/6 mice (6–8 weeks old, male) were purchased from Vital River Laboratory Animal Technology (Beijing, China). All animal experiments complied with the ARVO Statement for the Use of Animals in Ophthalmic and Vision Research and the guidelines of the Ethics Committee of Shandong Eye Institute. Type 1 DM was induced by intraperitoneal injection of streptozotocin (STZ, 50 mg/kg; Sigma-Aldrich, St. Louis, MO, USA) for 5 consecutive days. Mice with blood glucose levels exceeding 16.7 mmol/L were considered diabetic and were used for experiments 16 weeks after the final STZ injection. For IFN- $\gamma$  administration, healthy mice received injections of recombinant IFN- $\gamma$  (1  $\mu$ g/mL; Protein-tech, Shanghai, China) for 5 days, with normal saline as the vehicle control. To assess the effects of IFN- $\gamma$  blockage, anesthetized diabetic mice received subconjunctival injections of emapalumab (5  $\mu$ L, 1 mg/mL), an IFN- $\gamma$ -blocking antibody,<sup>33</sup> at 24 hours before, immediately before, and 24 hours after a 2.5-mm corneal epithelial scraping, with normal saline as the control.

### Corneal Sensitivity Measurement

Corneal sensitivity was assessed using a Cochet–Bonnet esthesiometer (Luneau Ophthalmologie, Chartres Cedex, France). Without anesthesia, the mice were gently restrained to fully expose the cornea. The central cornea was touched with a 60-mm-long nylon filament, which was gradually shortened in 5-mm increments until a blink reflex was elicited. The filament length at which the response occurred was recorded, and the final corneal sensitivity threshold was calculated as the average of three measurements.

## Tissue Preparation and Single Cell Isolation

Corneas from four diabetic mice (16 weeks post-STZ injection) and four age-matched control mice were excised and digested in Dispase II (Roche Diagnostics, Indianapolis, IN, USA) at 4°C for 18 hours to separate the corneal epithelium. The epithelium was further digested with trypsin (Sigma-Aldrich) at 37°C, and the remaining components of the cornea were digested with collagenase A (2.5 mg/mL; Roche Diagnostics) at 37°C for approximately 1 hour. During digestion, the suspensions were gently blown every 15 minutes until no tissue was visible under the microscope. The two single-cell suspensions were then combined and stained with Trypan blue (Sigma-Aldrich), and samples with >85% viability were subjected to 10x Genomics sequencing (10x Genomics, Pleasanton, CA, USA).

## Single-Cell RNA Sequencing and Data Processing

Single-cell suspensions were prepared for each sample, and libraries were generated using the 10x Genomics platform. Cells were partitioned to generate Gel Beads-in-Emulsion (GEMs), and barcoded cDNA libraries were constructed using the Single Cell 3' mRNA Kit (V2; 10x Genomics). Library quality was assessed using a Fragment Analyzer 2100 (Agilent Technologies, Santa Clara, CA, USA) before sequencing on the DNBSEQ platform (paired-end, 100-bp read length; MGI Tech, Shenzhen, China).

Read count matrices were generated using Cell Ranger (10x Genomics) counting and imported into the R Seurat 3.2.2 package (R Foundation for Statistical Computing, Vienna, Austria).<sup>34</sup> After quality control, the first 15 principal components (PCs) were used for clustering via the R FindClusters function at a resolution of 0.4 to yield 18 unsupervised cellular clusters. Clusters were visualized using Uniform Manifold Approximation and Projection (UMAP), for both individual and for samples. Immune cells were identified based on the immune cell-specific marker Ptpcr<sup>35</sup> and further subjected to unsupervised clustering. T cells were extracted using the T-cell-specific marker CD3.<sup>36,37</sup>

## Magnetic Bead Sorting for CD4<sup>+</sup>CD25<sup>–</sup> and CD8<sup>+</sup> T Cells

Spleens from 6- to 8-week-old mice were mechanically dissociated through a 40- $\mu$ m filter until no visible tissue remained. The filtrate was collected into a 15-mL centrifuge tube, treated with erythrocyte lysate (Beyotime, Shanghai, China), and counted. CD4<sup>+</sup>, CD4<sup>+</sup>CD25<sup>–</sup>, regulatory T cells (Tregs), and CD8<sup>+</sup> T cells were obtained using the Mouse CD4<sup>+</sup>CD25<sup>+</sup> Regulatory T Cell Isolation Kit and CD8a<sup>+</sup> T Cell Isolation Kit (Miltenyi Biotec, Bergisch Gladbach, Germany). Isolated cells were then cultured at a density of 10<sup>6</sup> cells/mL in Gibco RPMI 1640 medium (Thermo Fisher Scientific, Waltham, MA, USA) supplemented with Gibco anti-CD3/CD28 antibodies for three days to stimulate T cells.

## DC Isolation and Culture

The femur and tibia of 6- to 8-week-old male C57BL/6 mice were collected with bone marrow flushed by aspirating phosphate-buffered saline (PBS; Bioss Antibodies, Beijing, China) with a needle syringe and filtered through a 70- $\mu$ m filter. Erythrocyte lysate was then added. Leukocytes were subsequently obtained by centrifugation at

1000 rpm for 5 minutes in PBS. The cell pellet was resuspended in RPMI 1640 medium supplemented with 20-ng/mL granulocyte-macrophage colony-stimulating factor (GM-CSF; Novoprotein, Suzhou, China) and 10-ng/mL IL-4 (Novoprotein). RPMI 1640 medium with penicillin-streptomycin (HyClone Laboratories, Logan, UT, USA) and 10% Gibco fetal bovine serum (FBS) were added, and the cells were cultured in plates. After 3 days, the medium was replaced, and immature DCs were harvested on day 7. Mature DCs were generated by adding 100 ng/mL lipopolysaccharide (LPS; Sigma-Aldrich) and incubating for 12 hours.

### TG Neuron Cell Culture and Treatment

The eight-well glass chamber slides (Merck Millipore, Darmstadt, Germany) were coated with laminin (LN511; BioLamina, Sundbyberg, Sweden) and placed in a 37°C incubator for further use. Mouse trigeminal ganglia were isolated and processed under a microscope. The tissues were enzymatically digested with papain (Worthington Biomedical, Lakewood, NJ, USA) at 37°C for 20 minutes, followed by centrifugation to remove the supernatant. The samples were further digested at 37°C for 20 minutes with 4 mg/mL collagenase A (Roche, Mannheim, Germany). To separate myelin sheaths and nerve fragments from trigeminal neurons, a Percoll gradient was employed.<sup>38,39</sup> The gradient was prepared with 12.5% Percoll in the upper layer and 28% Percoll in the lower layer. The cell suspension was carefully layered on top of the gradient and subjected to gradient centrifugation at 2000 rpm for 35 minutes at 20°C, with slow acceleration from 0 followed by a slow deceleration back to 0. After centrifugation, the supernatant was discarded, and the cell sediment at the bottom of the tube was retained. The isolated cells were plated on laminin-coated eight-well glass chamber slides (Merck Millipore) and cultured in Gibco Neurobasal-A Medium containing B27 (STEMCELL Technologies, Vancouver, BC, Canada), penicillin-streptomycin (HyClone Laboratories), and 10% Gibco FBS. To exclude microglia effects, 2-μM PLX5622 (MedChemExpress, Monmouth Junction, NJ, USA) was added for 3 days, which eliminated >95% of the microglia.<sup>40</sup>

After overnight attachment, the TG neuron cells were co-cultured with the above isolated cultured cells, including immature DCs (iDCs), mature DCs (mDCs), activated CD8<sup>+</sup> T cells, and CD4<sup>+</sup>CD25<sup>+</sup> T cells, for 24 hours to assess their effects on neurite outgrowth. To investigate the impact of various factors on neurite outgrowth, TG neurons were cultured with 100-ng/mL recombinant IFN-γ (BioLegend, San Diego, CA, USA), 100-ng/mL recombinant IL-4 (Novoprotein), 100 ng/mL recombinant IL-17 (Novoprotein), and 100-μg/mL IFN-γ-blocking antibody (emapalumab; MedChemExpress).

### Immunofluorescence Staining

Following execution of the mice, the eyeballs were promptly removed and fixed on ice with 4% paraformaldehyde (PFA) for 1 hour. The corneas were then dissected and incubated overnight at 4°C in PBS containing 3% BSA and 0.3% Triton X-10. Subsequently, the corneas were incubated overnight at 4°C with fluorochrome-labeled antibodies: APC anti-mouse CD3 (100236; BioLegend), PE anti-mouse CD11c (117307; BioLegend), FITC anti-mouse CD4 (100405; BioLegend), Alexa Fluor 647 anti-Tubulin β 3 (801210; BioLegend), and rabbit Anti-CD8 alpha antibody

(ab217344; Abcam, Cambridge, UK). Corneas stained with anti-CD8 alpha antibody were incubated with Alexa Fluor 647-conjugated donkey anti-rabbit IgG (Invitrogen, Carlsbad, CA, USA) for 2 hours. The stained samples were visualized using an LSM 880 confocal microscope (Carl Zeiss Microscopy, Jena, Germany). To quantitatively analyze corneal nerves, an identical area of 0.75 mm<sup>2</sup> was selected in the central cornea of both control and diabetic mice. The ratio of the total nerve length in this region to the area it occupied was then calculated using ImageJ 1.54f (National Institutes of Health, Bethesda, MD, USA).<sup>41</sup>

To visualize neurite outgrowth, the cultured TG neurons were fixed with 4% PFA for 15 minutes, followed by 15 minutes of permeabilization with 0.3% Triton X-100. Thereafter, the cells were blocked with sheep serum (Boster Bio, Wuhan, China) for 1 hour and incubated with Anti-Beta III Tubulin Antibody, Alexa Fluor 488 Conjugate (AB15708A4; Sigma-Aldrich) for 1 hour at room temperature. Stained samples were imaged using an inverted microscope (Nikon, Tokyo, Japan), and the neurite length was analyzed using ImageJ software with the Simple Neurite Tracer (SNT) plugin.

### ELISA Analysis

Total protein was extracted from the corneas of diabetic mice and age-matched control mice. The IFN-γ concentration was measured using the Mouse IFN-gamma ELISA Kit – Quantikine (R&D Systems, Minneapolis, MN, USA), and the total tissue protein concentrations were quantified using a BCA protein assay kit (Jiangsu Aidisheng Biotechnology, Jiangsu, China), in accordance with the manufacturer's instructions.

### Statistical Analysis

All data were analyzed using Prism 8 (GraphPad Software, Boston, MA, USA). Two-tailed, unpaired Student's *t*-tests were employed to compare differences between two groups, and one-way ANOVA was used to compare differences between three or more groups. To ensure the reproducibility of results, data from this study are presented as mean ± standard deviation from at least three experiments. *P* < 0.05 was considered significant for all experiments performed. The raw sequence data for the control group and the DM group reported in this study were sourced from the GSE247392 dataset available in the Gene Expression Omnibus database (<https://www.ncbi.nlm.nih.gov/geo/>) and the CRA021135 dataset in the Genome Sequence Archive database (<https://ngdc.cnbc.ac.cn/gsa>), respectively.

## RESULTS

### DM Induced Corneal Nerve Degeneration in Mice

To replicate diabetic corneal nerve degeneration, we used type 1 diabetic mice induced by intraperitoneal injection of STZ according to our previous studies.<sup>11</sup> Four months after the final STZ injection, diabetic mice exhibited blood glucose levels above 30 mmol/L (Fig. 1A), restricted body weight (Fig. 1B), and reduced corneal sensitivity (Fig. 1C) compared to the age-matched healthy mice. To assess changes in corneal nerve density, whole-mounted corneal staining with anti-βIII-tubulin antibody was performed (Fig. 1D). Quantitative analysis revealed that the densities of both subbasal

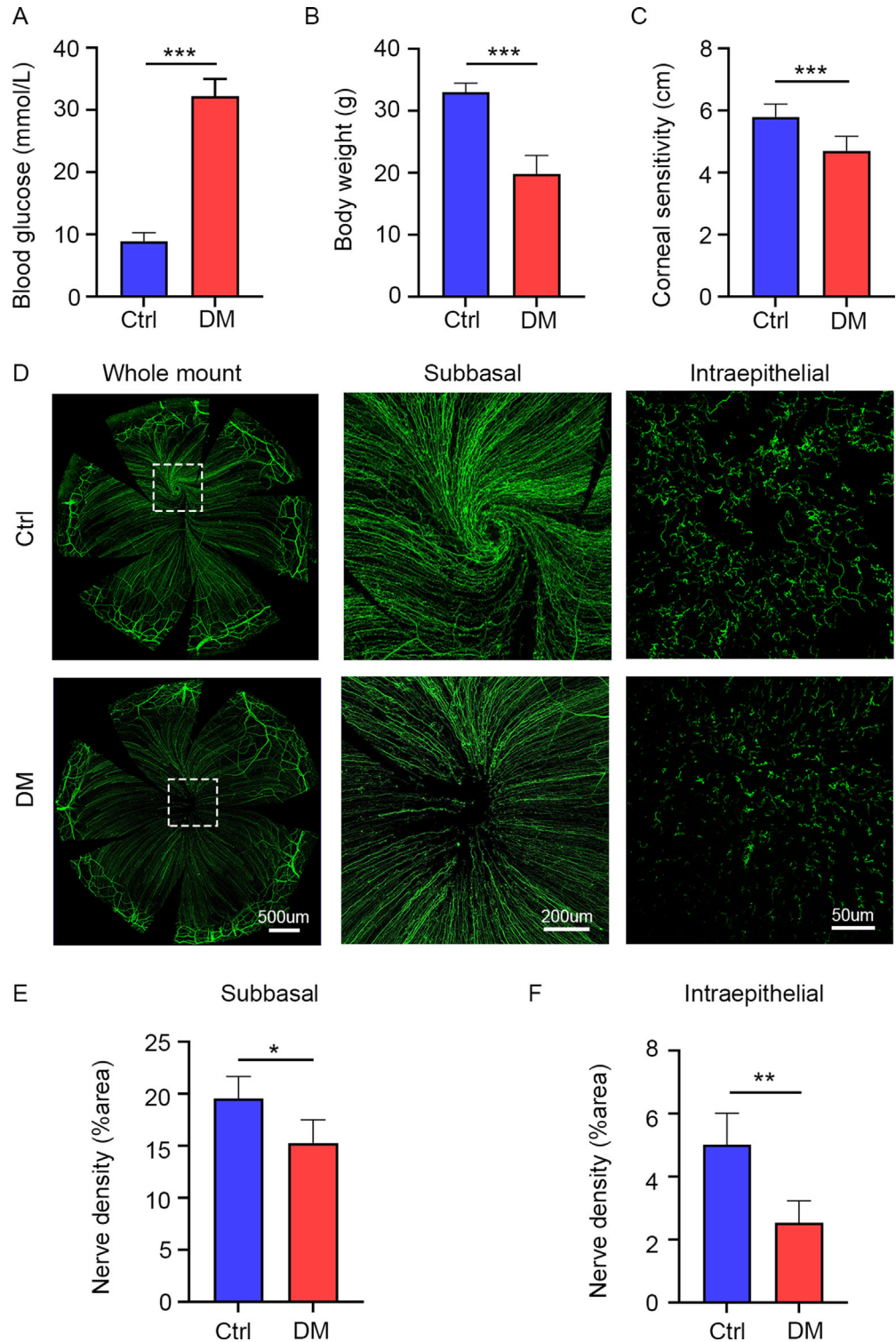


**FIGURE 1.** Identification of corneal nerve degeneration in diabetic mice. (A–C) Measurements of blood glucose, body weight, and corneal sensitivity in control (Ctrl) and DM mice ( $n = 20$  per group). (D) Representative image of whole-mounted corneal staining with anti- $\beta$ III-tubulin. (E) Comparison of corneal subbasal nerve density ( $n = 4$  per group). (F) Comparison of intraepithelial nerve terminals ( $n = 4$  per group). Data are presented as mean  $\pm$  SD; ns, not significant. \* $P < 0.05$ , \*\* $P < 0.01$ , \*\*\* $P < 0.001$ .

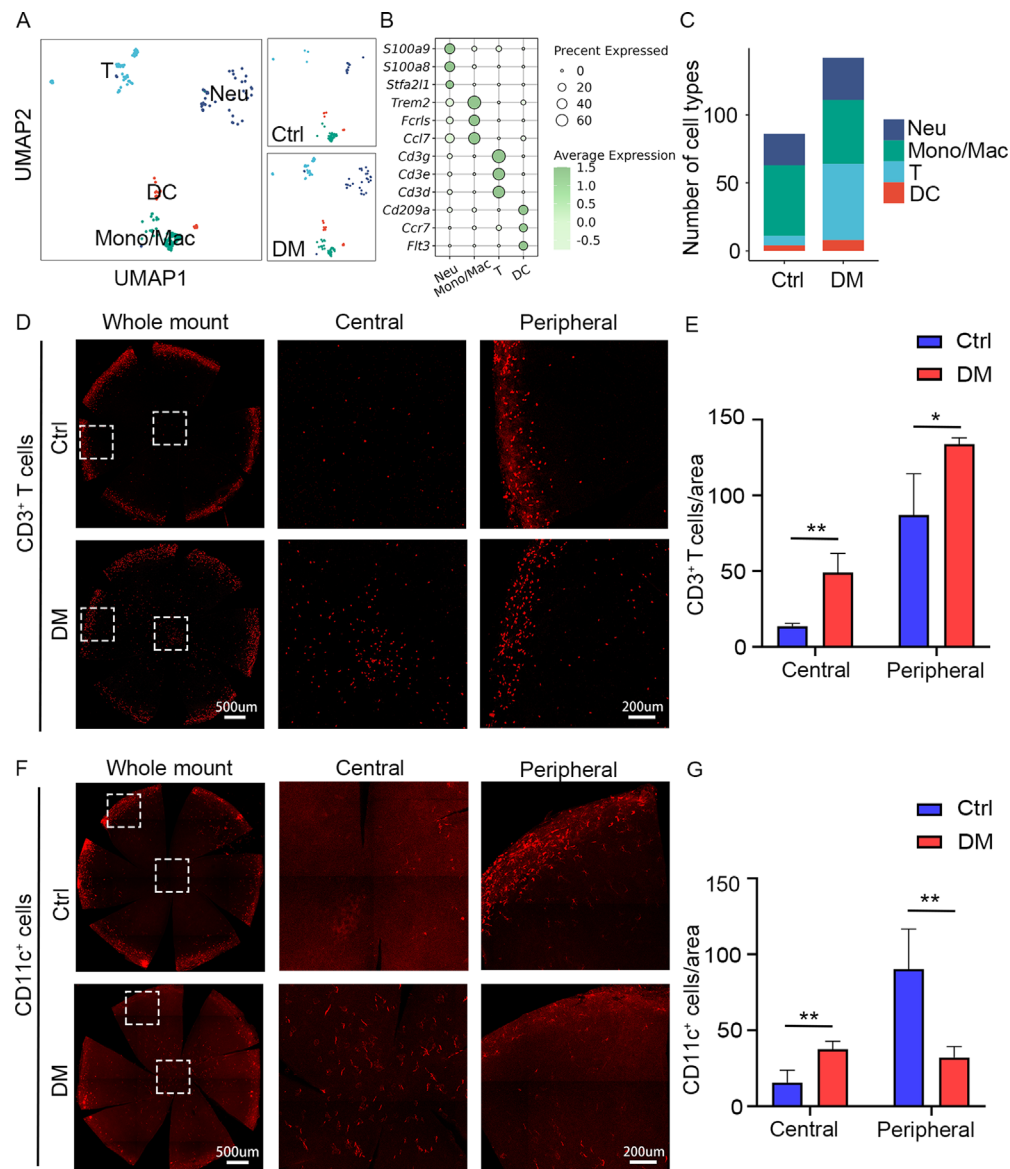


**FIGURE 2.** Alterations of DCs and T cells in diabetic cornea. **(A)** UMAP plots presenting cell types and groups. Neu, neutrophil; Mono/Mac, monocyte/macrophage; T, T cell; DC, dendritic cell. **(B)** Dot plot presenting expression of marker genes. **(C)** Alteration of the immune cell numbers between control (Ctrl) and DM corneas. **(D, E)** Representative images of CD3<sup>+</sup> T-cell staining and quantitative analysis between control and diabetic mouse corneas. **(F, G)** Representative images of CD11c<sup>+</sup> DC staining and quantitative analysis between control and diabetic mouse corneas ( $n = 4$  per group). Data are presented as mean  $\pm$  SD. \* $P < 0.05$ , \*\* $P < 0.01$ .

nerve fibers (Fig. 1E) and intraepithelial nerve terminals (Fig. 1F) were markedly reduced in diabetic mice compared with healthy mice. Comparatively, the reduction of intraepithelial nerve terminals was more significant than that of subbasal nerve density. These results indicate that diabetic mice exhibit similar characteristics of diabetic keratopathy, including corneal nerve degeneration and reduced corneal sensitivity.

### DM Altered Corneal DC and T-Cell Distribution in Mice

To gain insight into the composition and changes of corneal immune cells, we used scRNA-seq analysis of the immune cells from diabetic and age-matched healthy control mouse

corneas. According to the UMAP analysis, four distinct subpopulations (neutrophils, monocytes and macrophages, T cells, and DCs) were identified (Figs. 2A, 2B) with altered cellular composition (Fig. 2C). Compared with the slight increase of DCs, T cells increased most significantly in diabetic corneas. We further assessed the whole-mount corneal staining by using anti-CD11c and anti-CD3 antibodies to evaluate the alterations of DCs and T cells.<sup>21,42</sup> Similar to previous reports,<sup>43–45</sup> these two cells were predominantly located in the peripheral cornea, with a few cells in the central cornea of healthy mice. However, in diabetic mice, more DCs and T cells infiltrated into the central cornea (Figs. 2D, 2F). Quantitative analysis revealed that the number of CD3<sup>+</sup> T cells in the central and peripheral cornea of diabetic mice increased 3.7-fold and 1.5-fold, respectively, compared to control mice (central cornea:  $13 \pm 2$  cells in

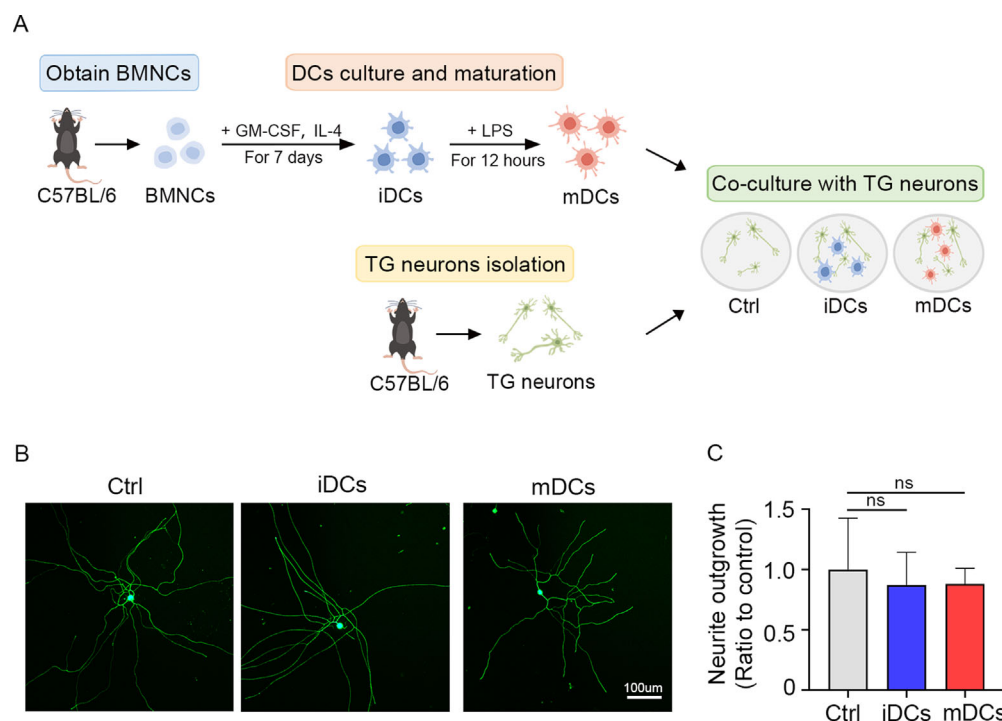


**FIGURE 3.** Co-culture of immature and mature DCs with TG neurons. **(A)** Schematic diagram of co-culture of TG neurons with iDCs and mDCs. **(B)** Representative images of TG neurite outgrowth co-cultured with iDCs and mDCs. **(C)** Quantitative analysis of TG neurite lengths ( $n = 6$  per group). Data are presented as mean  $\pm$  SD; ns, not significant.

control mice vs.  $49 \pm 12$  cells in diabetic mice; peripheral cornea:  $87 \pm 27$  cells in control mice vs.  $134 \pm 4$  cells in diabetic mice). Comparatively, the number of DCs marked by CD11c staining showed a modest elevation only in the central cornea ( $16 \pm 8$  cells in control mice vs.  $38 \pm 5$  cells in diabetic mice), with a decrease in the peripheral cornea ( $92 \pm 29$  cells in control mice vs.  $32 \pm 7$  cells in diabetic mice) (Figs. 2E, 2G). These findings suggest that CD3<sup>+</sup> T cells and CD11c<sup>+</sup> DCs infiltrate the central cornea in diabetic mice, which may contribute to nerve degeneration.

### DCs Exhibited No Significant Inhibition of TG Neurite Outgrowth

Immature and mature DCs reside in the healthy human cornea and have been reported to increase in diabetic conditions. To evaluate the potential role of DCs in diabetic corneal nerve degeneration, we isolated bone marrow-derived DCs and induced their maturation by LPS stimulation according to previous reports.<sup>46</sup> The maturation of DCs was confirmed by the morphologically roughened surfaces, emerging pseudopods, and higher major histocompatibility complex class II (MHC II) expression levels shown in flow cytometry analysis (Supplementary Figs. S1A, S1B).

Considering that neurons from healthy and diabetic mice might behave differently, we compared the healthy and diabetic TG neurons isolated and cultured in vitro. In the normal culture medium, the neurons displayed similar morphology and neurite outgrowth, whereas in the high-glucose medium the diabetic TG neurons were more sensitive and showed shorter neurite outgrowth. To study the cytokines that may impair the growth of TG neurites, we isolated TG neurons from healthy mice (Supplementary

Figs. S2A, S2B). The iDCs and LPS-induced mDCs were co-cultured with freshly isolated TG cells for 24 hours (Fig. 3A, Supplementary Fig. S1C). Neurite outgrowth was visualized using anti- $\beta$ III-tubulin staining and measured with ImageJ (Fig. 3B). Quantitative analysis showed that neither iDCs nor mDCs significantly inhibited TG neurite outgrowth compared with the control group without DCs (Fig. 3C). These results suggest that neither immature nor mature DCs exhibit significant effects in TG neurite outgrowth.

### Identification of Elevated T Cells in Diabetic Mouse Cornea

Based on the no significant inhibitory effect of DCs on TG neurite outgrowth, we next characterized the elevated T cells in diabetic corneas through scRNA-seq. The unbiased clustering approach identified four distinct clusters of corneal T cells, including CD4<sup>+</sup>CD25<sup>-</sup> T cells, CD8<sup>+</sup> T cells, Tregs, and  $\gamma\delta$ T cells (Fig. 4A). Quantitative analysis revealed that the number of CD4<sup>+</sup>CD25<sup>-</sup> T and CD8<sup>+</sup> T cells increased significantly in the diabetic cornea when compared with healthy cornea (Fig. 4B). The whole-mounted corneal staining was performed to verify the distribution of CD4<sup>+</sup> and CD8<sup>+</sup> T cells. Consistent with the distribution of CD3<sup>+</sup> T cells, the number of CD4<sup>+</sup> T cells in the peripheral cornea of diabetic mice was significantly higher than that of the control mice ( $63 \pm 16$  cells in control mice vs.  $129 \pm 34$  cells in diabetic mice). More importantly, CD4<sup>+</sup> T cells were detected in the central diabetic cornea when compared with no detection of CD4<sup>+</sup> T cells in the control central cornea (Figs. 4C, 4D). Paradoxically, we did not detect significant differences in the number of CD8<sup>+</sup> T cells between the peripheral and central cornea of control and diabetic mice by whole-mounted stain-

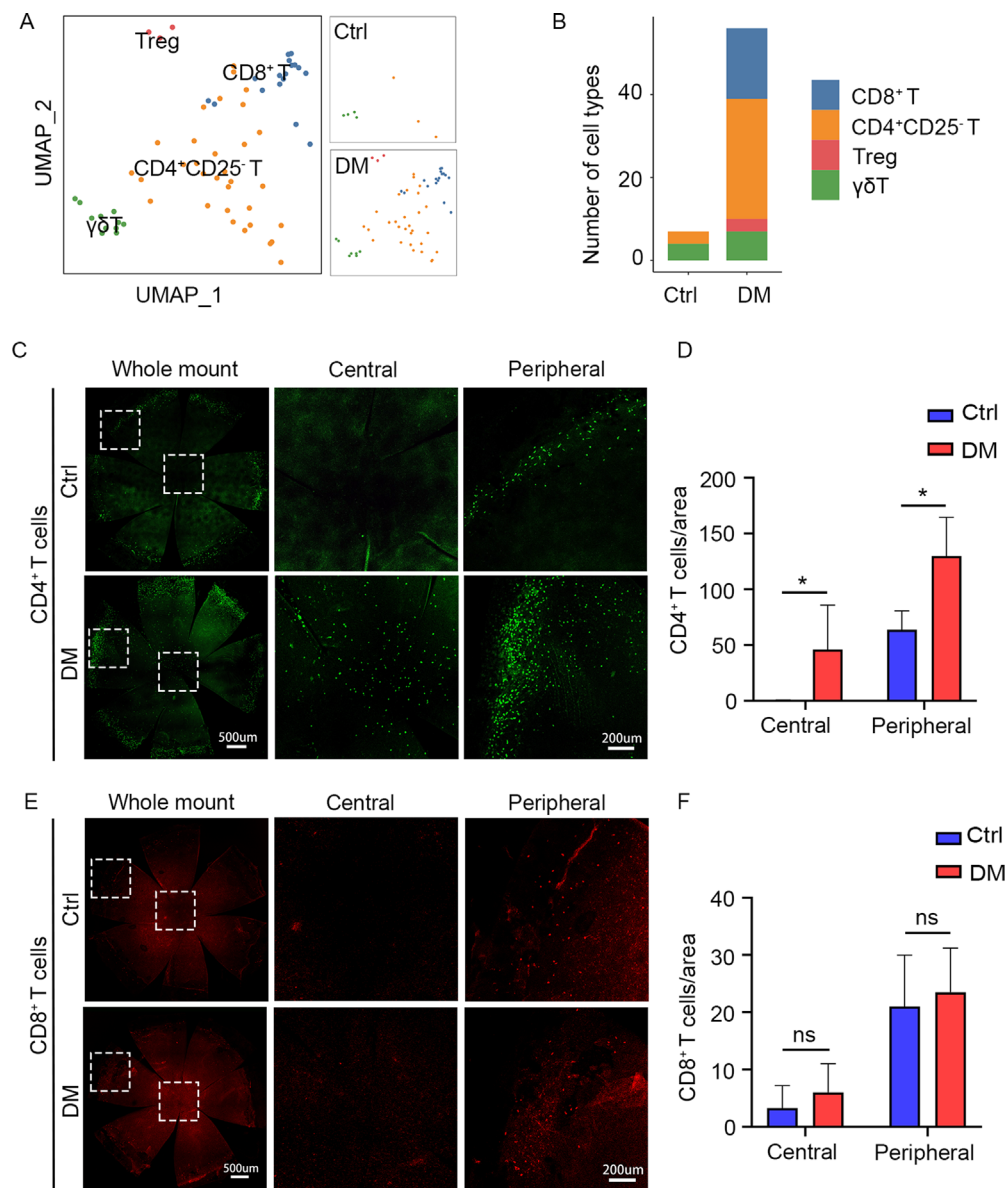


**FIGURE 4.** Alterations of T-cell subtypes in control and diabetic cornea. (A) UMAP plot analysis of T cells in control (Ctrl) and DM mouse corneas. (B) Bar plot presentation of the CD4<sup>+</sup>CD25<sup>-</sup> and CD8<sup>+</sup> T-cell numbers in control and diabetic mouse corneas. (C, D) Whole-mounted corneal staining and quantitative analysis of corneal CD4<sup>+</sup> T cells ( $n = 4$  per group). (E, F) Whole-mounted corneal staining and quantitative analysis of corneal CD8<sup>+</sup> T cells ( $n = 4$  per group). Data are presented as mean  $\pm$  SD; ns, not significant. \* $P < 0.05$ .

ing (central cornea:  $3 \pm 3$  cells in control mice vs.  $6 \pm 5$  cells in diabetic mice; peripheral cornea:  $21 \pm 9$  cells in control mice vs.  $26 \pm 8$  cells in diabetic mice), which was not consistent with the scRNA-seq results (Figs. 4E, 4F). Taken together, these single-cell RNA analysis and whole-mounted staining results suggest that CD4<sup>+</sup> T cells represent the predominantly increased T-cell type in the diabetic cornea.

#### CD4<sup>+</sup>CD25<sup>-</sup> T Cells But Not CD8<sup>+</sup> T Cells Inhibited TG Neurite Outgrowth

To discriminate the potential roles of different T cell subsets in TG neurite outgrowth, we purified CD4<sup>+</sup>CD25<sup>-</sup> and CD8<sup>+</sup> T cells from the spleen by magnetic bead sorting and

stimulated them with anti-CD3/CD28 antibodies in vitro. After 3 days of culture, these cells were co-cultured with mouse TG neurons for 24 hours (Fig. 5A). The outgrowth of TG neurites was visualized using anti- $\beta$ III-tubulin staining and measured with ImageJ (Fig. 5B). Quantitative analysis confirmed that only co-culture with activated CD4<sup>+</sup>CD25<sup>-</sup> T cells, but not CD8<sup>+</sup> T cells, led to significant inhibition of TG neurite outgrowth when compared with the anti-CD3/CD28 antibody treatment alone (Figs. 5B, 5C). These results indicate that CD4<sup>+</sup>CD25<sup>-</sup> T cells, but not CD8<sup>+</sup> T cells, inhibit TG neurite outgrowth. In addition, the scRNA-seq data showed that a small number of Tregs were newly generated in diabetic corneas, and these Tregs were found to promote the outgrowth of TG neurites when co-cultured with TG neurons in vitro (Supplementary Fig. S3).

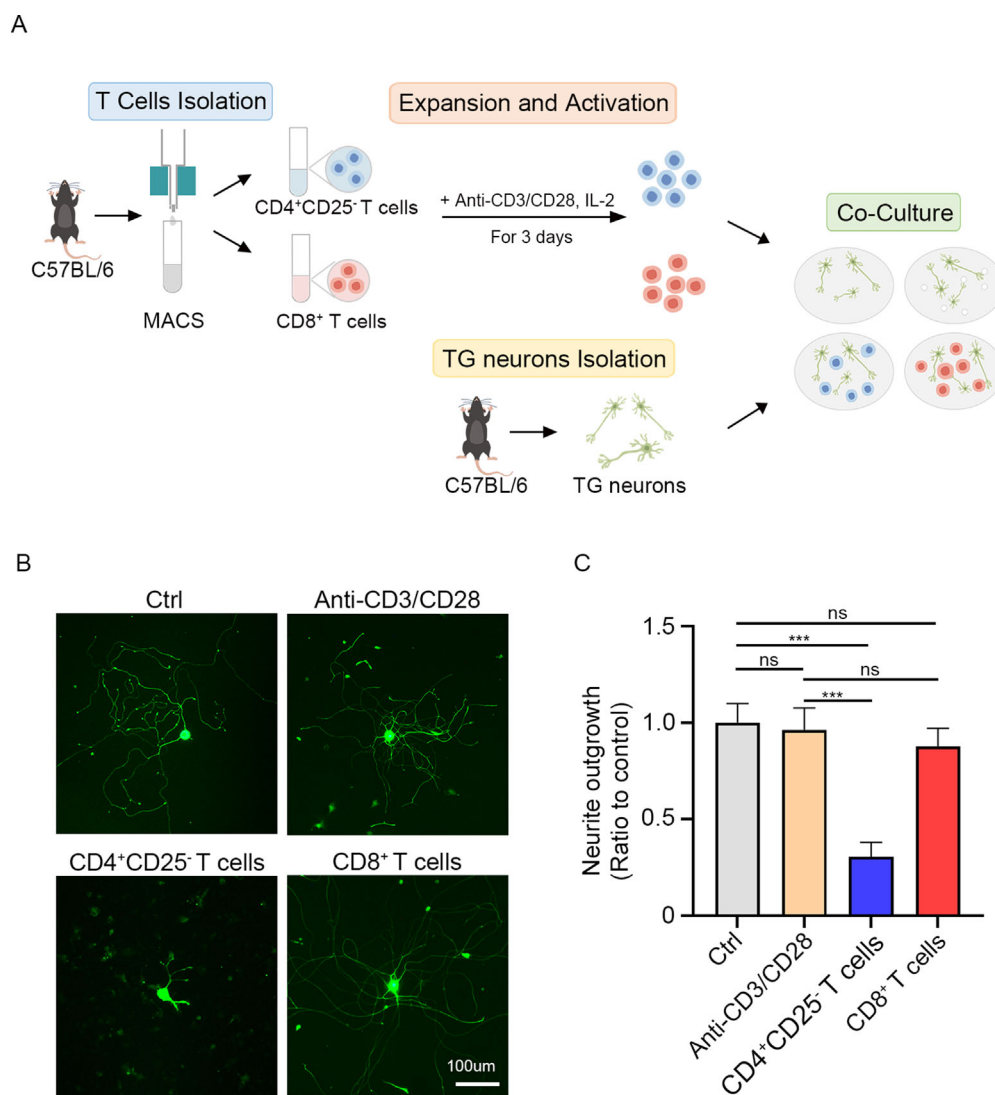


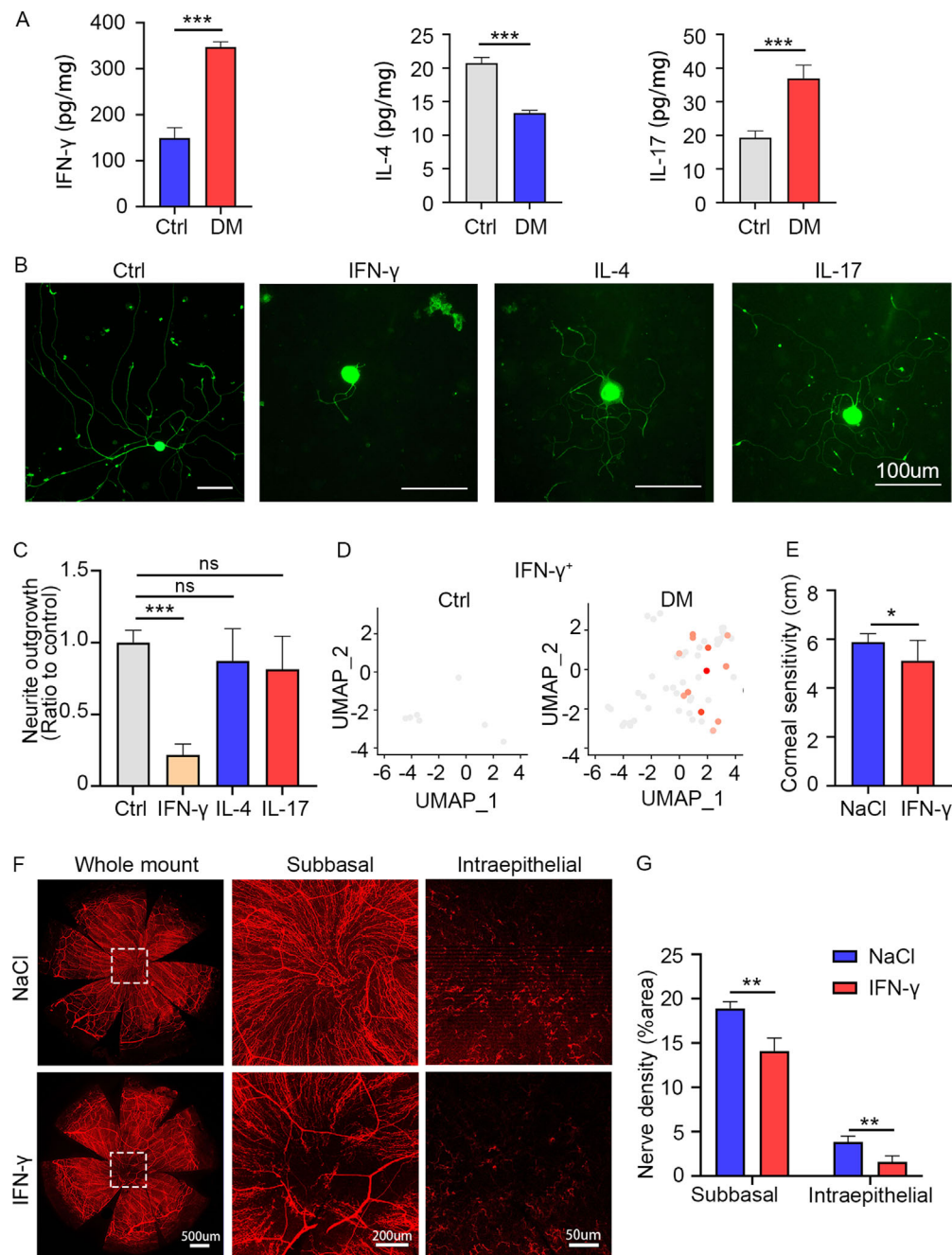
**FIGURE 5.** Co-culture of TG neurons with CD4<sup>+</sup>CD25<sup>-</sup> and CD8<sup>+</sup> T cells. **(A)** Schematic diagram of co-culture of TG neurons with CD4<sup>+</sup>CD25<sup>-</sup> T cells and CD8<sup>+</sup> T cells. **(B)** Representative images of TG neurite outgrowth co-cultured with CD4<sup>+</sup>CD25<sup>-</sup> T cells and CD8<sup>+</sup> T cells. **(C)** Quantitative analysis of TG neurite lengths ( $n = 4$  per group). Data are presented as mean  $\pm$  SD; ns, not significant. \*\*\* $P < 0.001$ .

### Involvement of IFN- $\gamma$ to the iNeurite Outgrowth and Corneal Nerve Degeneration

CD4<sup>+</sup> T cells exert their functions by secreting multiple cytokines, such as IFN- $\gamma$  from Th1 cells, IL-4 from Th2 cells, and IL-17 from Th17 cells.<sup>29–31</sup> Through ELISA assays, we found that IFN- $\gamma$  and IL-17 were elevated but IL-4 was reduced in the diabetic cornea (Fig. 6A). Additionally, in vitro experiments showed that IFN- $\gamma$  treatment, but not IL-4 or IL-17, significantly attenuated TG neurite outgrowth (Figs. 6B, 6C). We thus hypothesized that IFN- $\gamma$ , rather than IL-4 or IL-17, drives corneal nerve degeneration in diabetic mice. Furthermore, we assessed the respective influences of the increased inflammatory cytokines IL-1 $\beta$  and TNF- $\alpha$  in diabetic keratopathy<sup>20,40</sup> on the growth of TG neurons. The results showed that IFN- $\gamma$  and M1 macrophages had the most significant inhibitory effects compared to other factors (Supplementary Fig. S3).

To identify the role of IFN- $\gamma$  in corneal nerve degeneration, we reanalyzed the scRNA-seq data and found upreg-

ulated expression of IFN- $\gamma$  in CD4<sup>+</sup>CD25<sup>-</sup> T cells of the diabetic cornea (Fig. 6D), whereas other effector molecules were barely expressed (data not shown). To verify the potential involvement of IFN- $\gamma$  in corneal nerve degeneration, we subconjunctivally injected recombinant IFN- $\gamma$  into healthy mice for 5 days, with normal saline as the vehicle. The result showed that mice with the IFN- $\gamma$  injection exhibited significant reductions in corneal sensitivity, subbasal nerve density, and intraepithelial nerve terminal density (Figs. 6E–G). Furthermore, the addition of the IFN- $\gamma$ -blocking antibody emapalumab partially reversed the inhibition of TG neurite outgrowth that co-cultured with CD4<sup>+</sup>CD25<sup>-</sup> T cells (Figs. 7A, 7B). During corneal wound healing of diabetic mice, subconjunctival injection of emapalumab similarly promoted the regeneration of corneal subbasal and intraepithelial nerves (Figs. 7C, 7D). Furthermore, we investigated the possibility of IFN- $\gamma$  indirectly targeting microglia. After removing microglia with PLX5622 while culturing TG neurons, the addition of IFN- $\gamma$  also inhibited the outgrowth of TG neurites (Supplementary



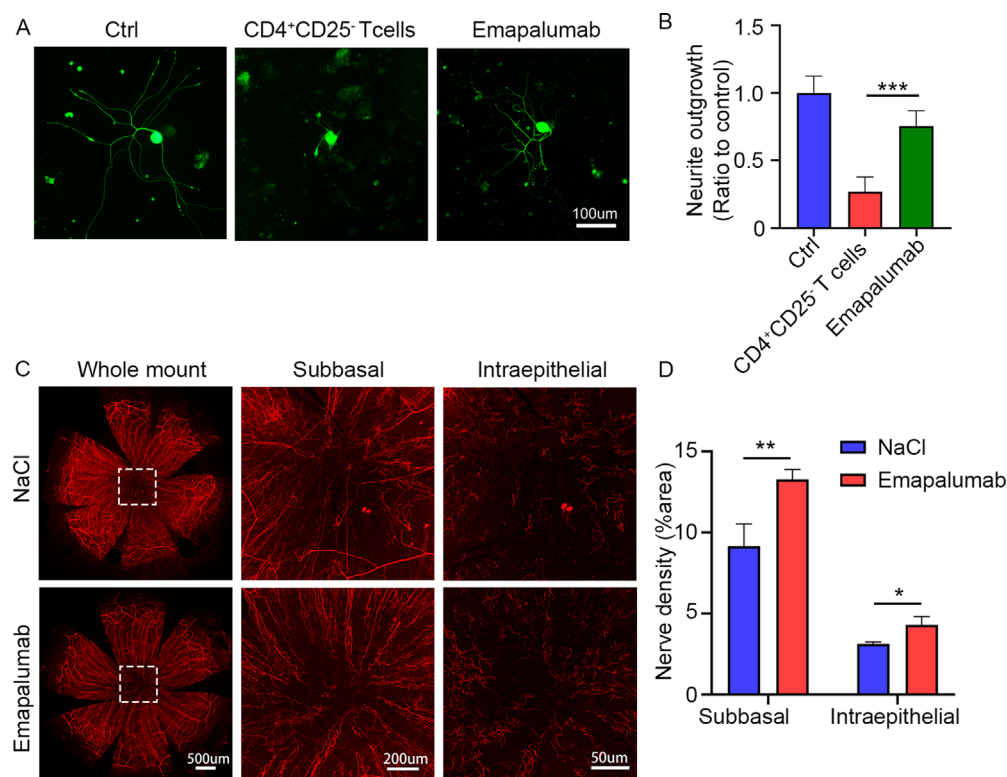
**FIGURE 6.** Effects of IFN- $\gamma$  on TG neurite outgrowth and corneal nerve degeneration. **(A)** ELISA analysis of IFN- $\gamma$ , IL-4, and IL-17 levels in control (Ctrl) and DM mouse cornea ( $n = 3$  per group). **(B, C)** Representative TG neuron staining images of Ctrl and groups treated with IFN- $\gamma$ , IL-4, or IL-17; the neurite lengths were analyzed using Image J ( $n = 3$  per group). **(D)** Feature plot analysis of IFN- $\gamma^{+}$  cells in control and diabetic mouse corneas. **(E)** Corneal sensitivity in mice treated with IFN- $\gamma$  ( $n = 8$  per group). **(F)** Whole-mounted corneal staining of vehicle and IFN- $\gamma$ -treated cornea. **(G)** Quantitative analysis of corneal nerve density ( $n = 4$  per group). Data are presented as mean  $\pm$  SD; ns, not significant. \* $P < 0.05$ ; \*\* $P < 0.01$ ; \*\*\* $P < 0.001$ .

Fig. S4). Therefore, these results suggest involvement of IFN- $\gamma$  secreted by CD4<sup>+</sup>CD25<sup>-</sup> T cells in the corneal nerve degeneration of diabetic mice.

## DISCUSSION

Diabetic keratopathy is characterized by corneal nerve degeneration and reduced sensitivity, which may lead to spontaneous corneal epithelial detachment and delayed

wound healing.<sup>5</sup> Most previous studies have focused on neuropeptides and neurotrophic factors to promote corneal epithelial and nerve regeneration. Accordingly, the important roles of several factors have been confirmed for the treatment of diabetic keratopathy, such as substance P, calcitonin gene-related peptide (CGRP), vasoactive intestinal peptide (VIP), nerve growth factor (NGF), mesencephalic astrocyte-derived neurotrophic factor (MANF), and vascular endothelial growth factor (VEGF).<sup>9–12</sup> However, the



**FIGURE 7.** Effects of IFN- $\gamma$  blockade on TG neurite outgrowth and corneal nerve degeneration. **(A, B)** Representative images and neurite length analysis of TG neurons co-cultured with CD4<sup>+</sup>CD25<sup>-</sup> T cells with or without the IFN- $\gamma$ -blocking antibody emapalumab ( $n = 4$  per group). **(C)** Whole-mounted staining of diabetic mouse corneas with epithelial injury after NaCl and emapalumab treatment. **(D)** Quantitative analysis of corneal subbasal and intraepithelial nerve density with NaCl and emapalumab treatment ( $n = 3$  per group). Data are presented as mean  $\pm$  SD. \* $P < 0.05$ , \*\* $P < 0.01$ , \*\*\* $P < 0.001$ .

mechanism of diabetic corneal nerve degeneration remains unclear. Using scRNA-seq analysis and whole-mounted corneal staining, we confirmed that multiple T cells infiltrated into the central cornea of the diabetic mice. Combining in vitro co-culture and in vivo animal experiments, we observed that CD4<sup>+</sup>CD25<sup>-</sup> T cells, rather than DCs or CD8<sup>+</sup> T cells, directly inhibited TG neurite outgrowth and promoted corneal nerve degeneration by secreting IFN- $\gamma$ .

Recent reports have identified several immune cells residing in the cornea, such as DCs, macrophages, mast cells, and lymphocytes.<sup>15,16</sup> These cells secrete different cytokines and growth factors, which function in the maintenance of corneal homeostasis and the response to pathological conditions.<sup>15</sup> Most previous studies have revealed the concomitant appearance of reduced nerve density and increased DCs in the diabetic human cornea. However, identifying other immune cells in the cornea is challenging using traditional corneal confocal microscopy. Therefore, we used scRNA-seq analysis and whole-mounted corneal staining to identify the changes in immune cell populations. The results revealed that the diabetic mice exhibited greater infiltration of DCs, CD4<sup>+</sup>, and CD8<sup>+</sup> T cells into the central cornea, consistent with the recent report of increased myeloid cell infiltration in both type 1 and type 2 diabetic mouse cornea.<sup>20</sup> Cytometry by time of flight (CyTOF) tests showed that there was no significant difference for CD4<sup>+</sup> T cells in the db/db mouse corneas, which may be related to the differences between type 1 and type 2 diabetic mice.<sup>47</sup> Moreover, previous studies confirmed the presence of CD4<sup>+</sup> and CD8<sup>+</sup> T cells in healthy mouse corneas,<sup>48</sup> whereas CD4<sup>+</sup> T-cell expansion has been found

in pathological conditions, such as immune rejection after corneal transplantation and herpes stromal keratitis.<sup>49,50</sup> Therefore, this evidence supports that DM promotes myeloid and lymphoid cell infiltration into the central cornea, which may be involved in the induction of diabetic corneal nerve degeneration.<sup>51,52</sup> In recent years, more reports have indicated the contribution of T cells in driving neurodegeneration, such as oligodendrocyte dysfunction, demyelination in the striatum and corpus callosum, and brain atrophy.<sup>53–55</sup> The pathological mechanism of diabetic corneal nerve degeneration remains unclear due to the complex microenvironment changes caused by hyperglycemia. Therefore, we adopted the in vitro co-culture model of immune cells with TG neurons to evaluate the effects of DCs and T cells on TG neurite outgrowth. The results found that CD4<sup>+</sup>CD25<sup>-</sup> T cells impaired TG neurite outgrowth, whereas DCs and CD8<sup>+</sup> T cells showed no significant impairment. The impacts of CD4<sup>+</sup> T cells on corneal neuropathy were similarly reported in dry eye disease, HSV-1 infection, and graft-versus-host disease.<sup>26,56,57</sup> It should be mentioned that a recent study using in vivo functional confocal microscopy found T cells residing in healthy human corneas, characterized by rapid, sustained movements and interactions with corneal dendritic cells and sensory nerves.<sup>16</sup> These findings provide potential evidence of CD4<sup>+</sup> T cells acting on corneal sensory nerves. Combined with our scRNA-seq analysis and in vitro co-culture results, we suggest that CD4<sup>+</sup> T cells represent the effector cells of driving corneal nerve degeneration in diabetic mice, whereas the antigen-presenting DCs may be essential for the activation of T cells.<sup>58</sup>

CD4<sup>+</sup> T cells mainly secrete IFN- $\gamma$ , IL-4, and IL-17 to coordinate immune responses in tissues.<sup>59,60</sup> Here we found that IFN- $\gamma$  level was increased in diabetic corneal CD4<sup>+</sup> T cells, which inhibited TG neurite outgrowth. Moreover, subconjunctival injection of IFN- $\gamma$  promoted corneal nerve degeneration in healthy mice, whereas IFN- $\gamma$  blockage promoted corneal nerve regeneration in diabetic mice. IFN- $\gamma$  is abundantly released by macrophages, activated CD8<sup>+</sup> T cells, natural killer T cells, and Th1 CD4<sup>+</sup> T cells.<sup>61</sup> In the context of Th1 cells, IFN- $\gamma$  serves as the predominant cytokine driving the differentiation of naïve CD4<sup>+</sup> T cells toward the Th1 phenotype,<sup>62</sup> establishing a positive feedback mechanism that augments the Th1-mediated immune responses. It should be mentioned that the secretion of IFN- $\gamma$  and IL-4 is characteristic of Th1 and Th2 cells, respectively.<sup>63</sup> The functions of these cytokines directly enhance cell-mediated and humoral immunity.<sup>64</sup> Here, we also found increased IL-17 and reduced IL-4 levels in the diabetic mouse cornea. Combined with the upregulated inflammatory factors IL-1 $\beta$  and TNF- $\alpha$ , we further evaluated their individual effects on TG neurite outgrowth. The results confirmed that IFN- $\gamma$  exhibited the most significant inhibitory effects when compared with other factors, IL-4 and IL-17 had no significant inhibitory effects. A previous study also illustrated the interactions between macrophages and corneal nerves.<sup>20</sup> In our in vitro co-culture models, we confirmed that M1 macrophages, but not M2 macrophages, impaired TG neurite outgrowth. The scRNA-seq data also revealed newly generated Tregs in diabetic corneas, which were found to promote the outgrowth of TG neurites (Supplementary Fig. S3). In addition, we excluded the possibility of indirect targeting of IFN- $\gamma$  on microglia, as IFN- $\gamma$  similarly impaired TG neurite outgrowth after microglia depletion (Supplementary Fig. S4). In line with our findings, a previous study reported that corneal nerves were sensitive to immune-driven damage mediated by Th1 CD4<sup>+</sup> T cells, rather than Th2 or Th17 CD4<sup>+</sup> T cells.<sup>65</sup> Consistent with the present findings, previous studies have also shown the active involvement of IFN- $\gamma$  in the pathogenesis of neurodegeneration, acting directly on neurons or indirectly through microglia cells. It should be mentioned that the combination of various cells and factors may involve the nerve degeneration of diabetic corneas. Their complex interactions warrant further investigation, which may provide more targets and protective strategies for diabetic keratopathy.

In summary, the present study confirms that DM increases CD4<sup>+</sup>CD25<sup>-</sup> T-cell infiltration into the central cornea, which contributes to diabetic corneal nerve degeneration partially through the secreted IFN- $\gamma$ .

### Acknowledgments

The authors thank Chao Wei (State Key Laboratory Cultivation Base, Shandong Provincial Key Laboratory of Ophthalmology, Eye Institute of Shandong First Medical University, Qingdao, China) for helpful advice on the manuscript.

Supported by grants from the National Natural Science Foundation of China (82070927 and 82371029), Taishan Scholar Program (tstp20221163), Key Research and Development Program of Shandong Province (2021ZDSYS14), and Joint Innovation Team for Clinical and Basic Research (202405).

**Data Availability:** The raw sequence data of the Ctrl group and the DM group reported in this study were sourced from the

GSE247392 dataset available in the Gene Expression Omnibus (GEO) database (<https://www.ncbi.nlm.nih.gov/geo/>) and the CRA021135 in the Genome Sequence Archive (GSA) database (<https://ngdc.cncb.ac.cn/gsa>) respectively.

Disclosure: **Y. Lin**, None; **L. Yang**, None; **Y. Li**, None; **S. Dou**, None; **Z. Zhang**, None; **Q. Zhou**, None

### References

- Ogurtsova K, Guariguata L, Barengo NC, et al. IDF Diabetes Atlas: global estimates of undiagnosed diabetes in adults for 2021. *Diabetes Res Clin Pract.* 2022;183:109118.
- Tomic D, Shaw JE, Magliano DJ. The burden and risks of emerging complications of diabetes mellitus. *Nat Rev Endocrinol.* 2022;18:525–539.
- Yu FX, Lee PSY, Yang L, et al. The impact of sensory neuropathy and inflammation on epithelial wound healing in diabetic corneas. *Prog Retin Eye Res.* 2022;89:101039.
- Buonfiglio F, Wasilica-Poslednik J, Pfeiffer N, Gericke A. Diabetic keratopathy: redox signaling pathways and therapeutic prospects. *Antioxidants (Basel).* 2024;13:120.
- Priyadarsini S, Whelchel A, Nicholas S, Sharif R, Riaz K, Karamichos D. Diabetic keratopathy: insights and challenges. *Surv Ophthalmol.* 2020;65:513–529.
- Asiedu K, Dhanapalaratnam R, Krishnan AV, Kwai N, Poynten A, Markoulli M. Impact of peripheral and corneal neuropathy on markers of ocular surface discomfort in diabetic chronic kidney disease. *Optom Vis Sci.* 2022;99:807–816.
- Shaheen BS, Bakir M, Jain S. Corneal nerves in health and disease. *Surv Ophthalmol.* 2014;59:263–285.
- Zhou T, Lee A, Lo ACY, Kwok J. Diabetic corneal neuropathy: pathogenic mechanisms and therapeutic strategies. *Front Pharmacol.* 2022;13:816062.
- Zhang Y, Gao N, Wu L, et al. Role of VIP and Sonic Hedgehog signaling pathways in mediating epithelial wound healing, sensory nerve regeneration, and their defects in diabetic corneas. *Diabetes.* 2020;69:1549–1561.
- Wang X, Li W, Zhou Q, et al. MANF promotes diabetic corneal epithelial wound healing and nerve regeneration by attenuating hyperglycemia-induced endoplasmic reticulum stress. *Diabetes.* 2020;69:1264–1278.
- Yang L, Di G, Qi X, et al. Substance P promotes diabetic corneal epithelial wound healing through molecular mechanisms mediated via the neurokinin-1 receptor. *Diabetes.* 2014;63:4262–4274.
- Wang Y, Zhao X, Wu X, Dai Y, Chen P, Xie L. MicroRNA-182 mediates Sirt1-induced diabetic corneal nerve regeneration. *Diabetes.* 2016;65:2020–2031.
- D'Onofrio L, Kalteniece A, Ferdousi M, et al. Small nerve fiber damage and Langerhans cells in type 1 and type 2 diabetes and LADA measured by corneal confocal microscopy. *Invest Ophthalmol Vis Sci.* 2021;62:5.
- Xu J, Chen P, Yu C, Liu Y, Hu S, Di G. In vivo confocal microscopic evaluation of corneal dendritic cell density and subbasal nerve parameters in dry eye patients: a systematic review and meta-analysis. *Front Med (Lausanne).* 2021;8:578233.
- Liu J, Li Z. Resident innate immune cells in the cornea. *Front Immunol.* 2021;12:620284.
- Downie LE, Zhang X, Wu M, et al. Redefining the human corneal immune compartment using dynamic intravital imaging. *Proc Natl Acad Sci USA.* 2023;120:e2217795120.
- Wu M, Hill LJ, Downie LE, Chinnery HR. Neuroimmune crosstalk in the cornea: the role of immune cells in corneal nerve maintenance during homeostasis and inflammation. *Prog Retin Eye Res.* 2022;91:101105.

18. Liu F, Liu C, Lee IXY, Lin MTY, Liu YC. Corneal dendritic cells in diabetes mellitus: a narrative review. *Front Endocrinol (Lausanne)*. 2023;14:1078660.
19. Colorado LH, Beecher L, Pritchard N, et al. Corneal dendritic cell dynamics are associated with clinical factors in type 1 diabetes. *J Clin Med*. 2022;11:2611.
20. Surico PL, Narimatsu A, Forouzanfar K, et al. Effects of diabetes mellitus on corneal immune cell activation and the development of keratopathy. *Cells*. 2024;13:532.
21. Gao N, Yan C, Lee P, Sun H, Yu FS. Dendritic cell dysfunction and diabetic sensory neuropathy in the cornea. *J Clin Invest*. 2016;126:1998–2011.
22. Gao N, Lee P, Yu FS. Intraepithelial dendritic cells and sensory nerves are structurally associated and functional interdependent in the cornea. *Sci Rep*. 2016;6:36414.
23. Steinman RM. The dendritic cell system and its role in immunogenicity. *Annu Rev Immunol*. 1991;9:271–296.
24. Heras-Murillo I, Adán-Barrientos I, Galán M, Wculek SK, Sancho D. Dendritic cells as orchestrators of anti-cancer immunity and immunotherapy. *Nat Rev Clin Oncol*. 2024;21:257–277.
25. Benowitz LI, Popovich PG. Inflammation and axon regeneration. *Curr Opin Neurol*. 2011;24:577–583.
26. Royer DJ, Echegaray-Mendez J, Lin L, et al. Complement and CD4<sup>+</sup> T cells drive context-specific corneal sensory neuropathy. *eLife*. 2019;8:e48378.
27. Yun H, Yin XT, Stuart PM, St Leger AJ. Sensory nerve retraction and sympathetic nerve innervation contribute to immunopathology of murine recurrent herpes stromal keratitis. *Invest Ophthalmol Vis Sci*. 2022;63:4.
28. Vereertbrugghen A, Pizzano M, Cernutto A, et al. CD4<sup>+</sup> T cells drive corneal nerve damage but not epitheliopathy in an acute aqueous-deficient dry eye model. *Proc Natl Acad Sci USA*. 2024;121:e2407648121.
29. Zhu J, Yamane H, Paul WE. Differentiation of effector CD4 T cell populations. *Annu Rev Immunol*. 2010;28:445–489.
30. McAleer JP, Fan J, Roar B, Primerano DA, Denvir J. Cytokine regulation in human CD4 T cells by the aryl hydrocarbon receptor and GQ-coupled receptors. *Sci Rep*. 2018;8:10954.
31. Zang X, Chen S, Zhu J, Ma J, Zhai Y. The emerging role of central and peripheral immune systems in neurodegenerative diseases. *Front Aging Neurosci*. 2022;14:872134.
32. Qin L, Li Q, Wang L, Huang Y. Mass cytometry reveals the corneal immune cell changes at single cell level in diabetic mice. *Front Endocrinol (Lausanne)*. 2023;14:1253188.
33. Vallurupalli M, Berliner N. Emapalumab for the treatment of relapsed/refractory hemophagocytic lymphohistiocytosis. *Blood*. 2019;134:1783–1786.
34. Satija R, Farrell JA, Gennert D, Schier AF, Regev A. Spatial reconstruction of single-cell gene expression data. *Nat Biotechnol*. 2015;33:495–502.
35. Fan Q, Yan R, Li Y, et al. Exploring immune cell diversity in the lacrimal glands of healthy mice: a single-cell RNA-sequencing atlas. *Int J Mol Sci*. 2024;25:1208.
36. Menon AP, Moreno B, Meraviglia-Crivelli D, et al. Modulating T cell responses by targeting CD3. *Cancers (Basel)*. 2023;15:1189.
37. Chatenoud L, Bluestone JA. CD3-specific antibodies: a portal to the treatment of autoimmunity. *Nat Rev Immunol*. 2007;7:622–632.
38. Katzenell S, Cabrera JR, North BJ, Leib DA. Isolation, purification, and culture of primary murine sensory neurons. *Methods Mol Biol*. 2017;1656:229–251.
39. Malin SA, Davis BM, Molliver DC. Production of dissociated sensory neuron cultures and considerations for their use in studying neuronal function and plasticity. *Nat Protoc*. 2007;2:152–160.
40. Liu Y, Given KS, Dickson EL, Owens GP, Macklin WB, Bennett JL. Concentration-dependent effects of CSF1R inhibitors on oligodendrocyte progenitor cells ex vivo and in vivo. *Exp Neurol*. 2019;318:32–41.
41. Wang C, Fu T, Xia C, Li Z. Changes in mouse corneal epithelial innervation with age. *Invest Ophthalmol Vis Sci*. 2012;53:5077–5084.
42. Chetty R, Gatter K. CD3: structure, function, and role of immunostaining in clinical practice. *J Pathol*. 1994;173:303–307.
43. Hamrah P, Dana MR. Corneal antigen-presenting cells. *Chem Immunol Allergy*. 2007;92:58–70.
44. Altshuler A, Amitai-Lange A, Tarazi N, et al. Discrete limbal epithelial stem cell populations mediate corneal homeostasis and wound healing. *Cell Stem Cell*. 2021;28:1248–1261.e8.
45. Forrester JV, Xu H, Kuffová L, Dick AD, McMenamin PG. Dendritic cell physiology and function in the eye. *Immunol Rev*. 2010;234:282–304.
46. Biscari L, Kaufman CD, Farré C, et al. Immunization with lipopolysaccharide-activated dendritic cells generates a specific CD8<sup>+</sup> T cell response that confers partial protection against infection with *Trypanosoma cruzi*. *Front Cell Infect Microbiol*. 2022;12:897133.
47. Furman BL. Streptozotocin-induced diabetic models in mice and rats. *Curr Protoc Pharmacol*. 2015;70:5.47.41–45.47.20.
48. Mott KR, Osorio Y, Brown DJ, et al. The corneas of naive mice contain both CD4<sup>+</sup> and CD8<sup>+</sup> T cells. *Mol Vis*. 2007;13:1802–1812.
49. Wang S, Mittal SK, Lee S, et al. Effector T cells promote fibrosis in corneal transplantation failure. *Invest Ophthalmol Vis Sci*. 2024;65:40.
50. O'Neil TR, Hu K, Truong NR, et al. The role of tissue resident memory CD4 T cells in herpes simplex viral and HIV infection. *Viruses*. 2021;13:359.
51. Donath MY, Shoelson SE. Type 2 diabetes as an inflammatory disease. *Nat Rev Immunol*. 2011;11:98–107.
52. Lee EJ, Rosenbaum JT, Planck SR. Epifluorescence intravital microscopy of murine corneal dendritic cells. *Invest Ophthalmol Vis Sci*. 2010;51:2101–2108.
53. Chen X, Firulyova M, Manis M, et al. Microglia-mediated T cell infiltration drives neurodegeneration in tauopathy. *Nature*. 2023;615:668–677.
54. Gao C, Jiang J, Tan Y, Chen S. Microglia in neurodegenerative diseases: mechanism and potential therapeutic targets. *Signal Transduct Target Ther*. 2023;8:359.
55. Berriat F, Lobsiger CS, Boillée S. The contribution of the peripheral immune system to neurodegeneration. *Nat Neurosci*. 2023;26:942–954.
56. Yun H, Yee MB, Lathrop KL, Kinchington PR, Hendricks RL, St Leger AJ. Production of the cytokine VEGF-A by CD4<sup>+</sup> T and myeloid cells disrupts the corneal nerve landscape and promotes herpes stromal keratitis. *Immunity*. 2020;53:1050–1062.e5.
57. Vereertbrugghen A, Pizzano M, Cernutto A, et al. CD4<sup>+</sup> T cells drive corneal nerve damage but are dispensable for corneal epitheliopathy development in dry eye disease. *bioRxiv*. 2024. <https://doi.org/10.1101/2024.03.22.586336>.
58. Hilligan KL, Ronchese F. Antigen presentation by dendritic cells and their instruction of CD4<sup>+</sup> T helper cell responses. *Cell Mol Immunol*. 2020;17:587–599.
59. Annunziato F, Romagnani C, Romagnani S. The 3 major types of innate and adaptive cell-mediated effector immunity. *J Allergy Clin Immunol*. 2015;135:626–635.
60. Hirahara K, Nakayama T. CD4<sup>+</sup> T-cell subsets in inflammatory diseases: beyond the Th1/Th2 paradigm. *Int Immunol*. 2016;28:163–171.

61. Bhat P, Leggatt G, Waterhouse N, Frazer IH. Interferon- $\gamma$  derived from cytotoxic lymphocytes directly enhances their motility and cytotoxicity. *Cell Death Dis.* 2017;8:e2836.
62. Schroder K, Hertzog PJ, Ravasi T, Hume DA. Interferon- $\gamma$ : an overview of signals, mechanisms and functions. *J Leukoc Biol.* 2004;75:163–189.
63. Morinobu A, Kumagai S. [Cytokine measurement at a single-cell level to analyze human Th1 and Th2 cells]. *Rinsho Byori.* 1998;46:908–914.
64. Paludan SR. Interleukin-4 and interferon- $\gamma$ : the quintessence of a mutual antagonistic relationship. *Scand J Immunol.* 1998;48:459–468.
65. Vereertbrugghen A, Pizzano M, Sabbione F, et al. An ocular Th1 immune response promotes corneal nerve damage independently of the development of corneal epitheliopathy. *J Neuroinflammation.* 2023;20:120.